Positron scattering from ethane

Ryan Stocks (u6311272)

2nd Year Physics, 1st Physics ASC

Supervised by Dr. James Sullivan

Abstract

The interaction of antimatter with matter and its apparent rarity has intrigued physicists ever since antimatter was discovered in the early 20th century. Positron scattering from molecules is particularly interesting as it has important applications in medical imaging and atomic physics [1, 2, 3]. Recent developments in theory have successfully predicted positron bound state energies for larger alkane molecules, however they do not predict bound states for ethane contrary to experimental evidence [4, 5]. Experimental results published to date for positron-ethane interactions have probed no deeper than the total cross section. This report extends existing experimental results by detailing methodology to additionally separate the total cross section into positronium formation and difference (combined elastic and inelastic scattering) components. This is achieved by containing the apparatus in an ∼0.05 T magnetic field which allows the separation of scattered positrons due to a shift in their parallel versus perpendicular energy.

Measurements of the grand total, positronium formation, and difference cross sections for a positron-ethane interaction are reported in the energy range from 1 to 100 eV. A comparison is made with previous grand total cross sections results, with the new experimental data consistent with the previous work of Chiari et. al. [6] and Floeder et. al. [7]. The separation of the ethane grand total cross section into positronium formation and difference components presents novel work. The positronium cross section is zero below the calculated positronium formation threshold of 4.7 eV and reaches a maximum of 7.9 ± 0.3 Å^2 at 15 eV before declining at higher energies. The difference cross section is maximal at low energies, decreasing until the peak of the positronium formation cross section and then increasing again at higher energies, likely due to having sufficient energy to inelastically excite higher energy states or ionize the ethane molecule. Systematic errors were observed in the cross section measurements and further work will be required to reduce these errors and obtain publishable results; however, this was beyond the time scope of this project.

Introduction

The existence of the antielectron or positron (e^+) was predicted by Paul Dirac in 1928 when reconciling quantum theory with special relativity to describe the behaviour of electrons [8]. They were first observed and identified in a cloud chamber by Carl Anderson later in 1932 [9]. Since then, several antimatter particles have been artificially produced and studied including antiprotons and anti-hydrogen in small quantities [10, 11]. The study of antimatter has been vital to the analysis of cosmic radiation [1] and many applications have been developed utilising these particles. This includes Positron Annihilation Spectroscopy (PAS) for studying material structure [2] and Positron Emission Topography (PET) for medical imaging [3]. Further study of antimatter and its interactions with matter will assist the advancement of quantum theory and may help explain the matter-antimatter asymmetry.

Positron scattering or the interaction of positrons with matter is an interesting problem in antimatter physics. It is vital to applications such as PAS and PET but has proven difficult for theory as it forms an intractable n-body problem for larger molecules. An intriguing property of these interactions not yet evident in *ab initio* theory is the existence of positron-molecule bound states. The existence of these bound states is evident due to significantly increased annihilation cross sections at low energies relative to that predicted from the electron density alone indicating resonances. A bound state or associated resonance would justify the enlarged cross section as positron binding would provide increased contact time for annihilation. Various attempts of ranging success have been made to integrate bound states with existing theory. A recent attempt by Swann and Gribakin [5] adds a parameterized potential describing the polarization of the electron cloud. This attempt has proven to align well with experimental results for the positron binding energy of larger alkane molecules. However, contrary to experimental results, this theory does not predict a bound state for ethane (C_2H_6). The annihilation cross-section of positron-ethane at low energies is significantly larger than expected. It peaks around the ~370 meV [12] vibrational modes as shown in Figure 1 from Gilbert et. al. [4]. This is consistent with a resonance state where excess energy of the positron is temporarily transferred to molecular vibrations. Ethane is thus of particular interest for further research as this apparent bound state is not yet well understood.

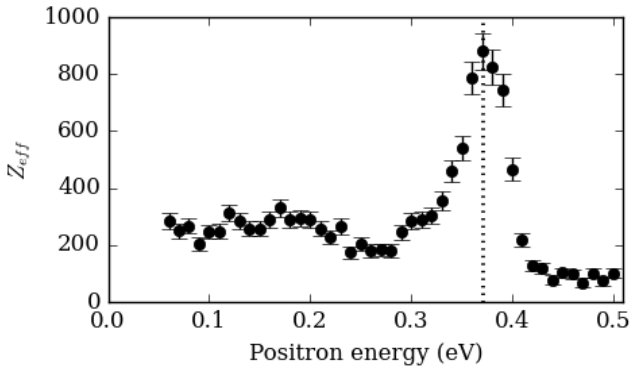

Figure 1: Annihilation rate as a function of positron energy for ethane by Gilbert et. al. [4]. Z_{eff} is a dimensionless parameter relating the cross section to that of an uncorrelated electron gas of equivalent numeric density. The dashed vertical line indicates the ~370 meV vibrational modes.

To provide a comprehensive picture of the behaviour of positron scattering from ethane, a collection of cross section measurements must be accumulated. This report will detail measurements of the grand total, positronium formation and difference (combined elastic and inelastic scattering) cross sections for positron-ethane at collision energies between 1 and 100 eV. This will form part of a broader project investigating positron-ethane scattering to probe the bound states and resonances described above and will help ensure the apparatus is functioning correctly. Two previous experimental studies of the grand total cross section for positron-ethane are known, which will provide a good consistency check. These studies were conducted by Floeder et. al. in the energy range 5 to 400 eV [7] and Chiari et. al. in the energy range 0.1 to 70 eV [6]. The two studies used similar apparatus with electrostatic beam optics and their results align well over the common energy range from 5 to 70 eV. This study takes a fundamentally different approach, with the entire positron beam contained in a ~0.05 T magnetic field. This allows the positronium formation component of the cross section to be separated as described in the method section below. There are no known previous studies of the positronium, elastic, or inelastic scattering cross sections of positrons with ethane.

As the full experiment is contained in a magnetic field, the field will exert a force on the positrons. The force on a particle with charge q travelling with velocity $\boldsymbol{v}$ in a uniform magnetic field $\boldsymbol{B}$ is

$$\boldsymbol{F} = q\boldsymbol{v} \times \boldsymbol{B} \tag{1}$$

which is perpendicular to both the motion of the particle and the magnetic field. This causes the charged particle to follow a helical path in the direction of the magnetic field. This can be used to guide the positrons through the experiment. The velocity of the particle can be split into a velocity parallel to the magnetic field $v_{\parallel}$ and a velocity perpendicular to the magnetic field $v_{\perp}$. The energy can likewise be split into parallel and perpendicular components such that the total energy is the sum of the two

$$E = E_{\perp} + E_{\parallel} \tag{2}$$

Since the parallel component of the velocity does not affect the force on the particle, the force is only dependent on the perpendicular component. The radius of the helical path is known as the cyclotron radius and can be calculated as

$$r_c = \frac{mv_{\perp}}{|qB|} = \frac{\sqrt{2mE_{\perp}}}{|qB|} \tag{3}$$

Since the positrons follow the magnetic field, this means that as a positron moves from a weaker magnetic field to a stronger magnetic field, both the spot size (spread of the positrons) and the cyclotron radius is decreased.

When a positron collides with a molecule, there are four potential outcomes. First, it may scatter elastically at an angle θ from its initial trajectory. In this case little energy is transferred between the positron and the target particle due to conservation of momentum and the significant difference in mass. Assuming that the initial velocity of the positron is primarily parallel to the magnetic field ($E \approx E_{\parallel}$), the parallel energy following the collision can be calculated from the scattering angle θ

$$E'_{\parallel} = E\cos^2\theta \tag{4}$$

where E is the initial energy of the positron and $E'_{\parallel}$ is the energy of the positron in the parallel direction following the collision. The scattering angle θ can hence be calculated from the change in parallel energy

$$\theta = \cos^{-1}\left(\sqrt{\frac{E'_{\parallel}}{E}}\right) \tag{5}$$

Second, the positron may transfer energy to the target molecule exciting or ionizing the molecule and scattering with reduced energy which is referred to as inelastic scattering. The difference cross section in this study will represent the combination of both the elastic and inelastic cross sections.

Third, the positron may annihilate with one of the electrons in the molecule. This annihilation most commonly produces 2 photons with a characteristic energy of 511 keV each ($m_e c^2$ where m_e is the mass of the positron/electron) but can also produce 3 photons each with a total energy of 1022 keV.

Finally, if the positron has sufficient energy it can bind with one of the electrons in the molecule and form positronium. Positronium is a short-lived neutral particle that will annihilate to produce 2 or 3 photons after $0.1 - 140$ ns depending on the spin alignment of the positron and electron [13]. Ethane has an ionisation energy of approximately $E_{ion} = 11.5$ eV [14] so the minimum collision energy required for positronium formation is expected to be $E_{ps} = E_{ion} - 6.8\,eV = 4.7$ eV where 6.8 eV is the binding energy for positronium [15]. In general, the positronium formation cross section is 5 orders of magnitude larger than the annihilation cross section so the direct annihilation component is considered negligible in this study.

To describe the probability of a particular interaction between particles, physicists primarily use the cross section, σ. The cross section can be thought of as description of the interaction probability of two incident particles. This probability can be dependent on the particle energies for quantum systems. The cross section can be used to relate the relative probabilities of different interactions, including positronium formation or annihilation in the case of a positron-molecule collision system. In addition to total cross sections, a differential

cross section can be used to relate the cross section to the angle that a particle scatters. The differential cross section is typically written as

$$\frac{d^2\sigma}{dE'd\Omega}(E, E', \Omega) \tag{6}$$

where E is the initial kinetic energy, E' is the final kinetic energy after the interaction and $d\Omega$ describes the solid angle at which the particle is scattered as illustrated in Figure 2. The apparatus described in the method section below can also be used to measure differential elastic and differential in-elastic cross sections. This was unfortunately beyond the time scope of this project however it will form interesting future work, particularly to investigate the inelastic cross sections around the 370 meV vibrational mode described above.

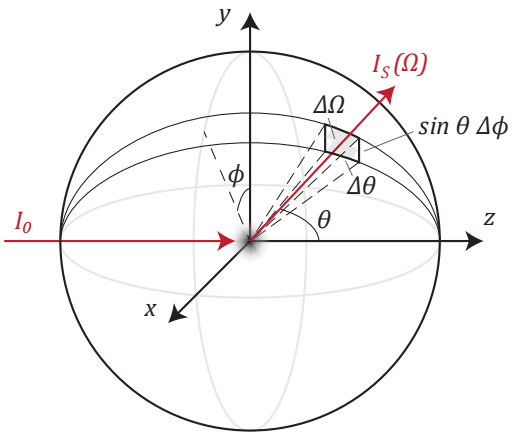

Figure 2: Illustration of the differential cross section for an incident beam with intensity I_0 scattering into the solid angle $\Delta\Omega = \sin\theta\,\Delta\theta\,\Delta\phi$ with intensity $I_S(\Omega)$.

Method

The experimental apparatus has been described in detail previously [16] so a summary of the most important details is contained below followed by a description of the analysis techniques. A schematic of the full experimental apparatus is provided in Figure 3.

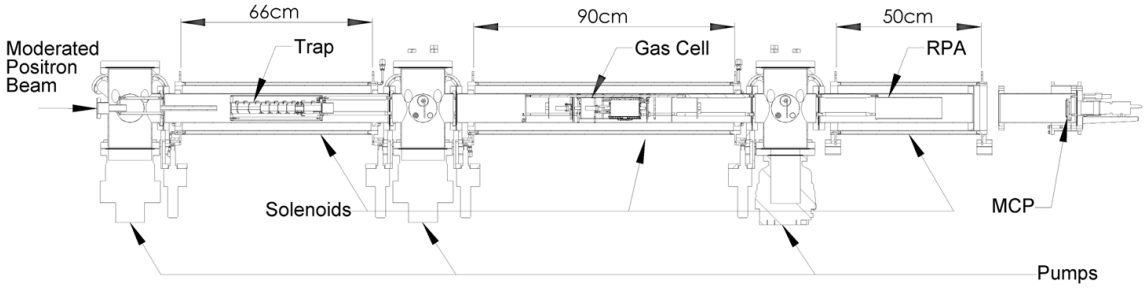

Figure 3: Schematic of experimental apparatus showing the layout of the trap, gas scattering cell, vacuum pumps, and retarding potential analyser (RPA) along with the positions of the vacuum pumps, solenoids, and multichannel plate detector (MCP)

High energy positrons (hundreds of keV) are obtained from a sample of the radioactive isotope sodium-22. This synthetic isotope decays via β^+ positron emission to neon-22 with a half-life of 2.6 years (current activity ~45 mCi). The sodium sample is positioned between two Helmholtz coils to provide a consistent 0.018 T magnetic field guiding the positrons. The positrons pass through a moderator consisting of a copper cone cooled to ~7 K and coated in a thin layer of solid neon. Most positrons annihilate in transit through the neon, however approximately 1% of the positrons are ejected with a significantly reduced kinetic energy of ≈ 2 eV [17].

The moderated positrons are accelerated with an electronic potential (33 V) and guided magnetically into a penning trap consisting of nine cylindrical electrodes in a stronger 0.05 T magnetic field. The stronger magnetic field compresses the positrons radially producing a tighter beam. The electrodes are set to form a sequence of seven potential steps to trap the positrons as they are slowed by a sequence of inelastic collisions with a nitrogen (N_2) and carbon tetrafluoride (CF_4) buffer gas. The first collision excites one of the electronic states of the nitrogen molecule (~8.3 eV) which reduces the kinetic energy of the positron sufficiently to trap it in the potential well. A sequence of further inelastic collisions exciting vibrational and rotational states of N_2 and CF_4 reduces the energy of the positron further until it is confined in the final potential well. It is then cooled to room temperature ($\frac{3}{2}kT \approx 0.04$ eV) over approximately 3 ms. The gas pressure is reduced in the later potential steps using differential pumping to increase the lifetime of the trapped positrons.

Once positrons have accumulated in the trap (approximately 100 times per second), a pulsed beam of positrons is released by gradually increasing the potential in the final well of the trap. This gives the positrons sufficient energy to "spill over" the barrier at the end of the trap. This produced a beam with an energy width of $\Delta E = 50$ meV (full width at half maximum). The height of the trap barrier defines the transport energy E_T of the positron which was 100 eV for all experiments presented here. They were then accelerated and magnetically guided into the scattering cell, which contains the target gas (in this case ethane). By accelerating the positrons in the parallel direction only, the ratio of the cyclotron period to the cyclotron radius is increased significantly causing the positrons to scatter as though they are a parallel rather than helical beam. The scattering cell is a 50 ± 0.25 mm long gold coated copper cylinder with 5 mm apertures at either end providing both a uniform potential and gas pressure. The potential of the scattering cell defines the energy of the energy of the positron-ethane collision. By setting the scattering cell potential $V_{SC} = \frac{E_T - E}{e}$ the positron will have a kinetic energy E within the cell. This allows the transport energy of the positron E_T to remain constant for all tests. The pressure of the target gas in the scattering cell is measured and recorded by a MKS Baratron capacitance manometer with an absolute uncertainty of ~1% or ± 0.003 mTorr in the range considered.

Following the scattering cell is a retarding potential analyser (RPA) which can filter positrons based on their parallel energy ($E_\parallel$). When positrons scatter either elastically or inelastically, the parallel energy is decreased and as a result can be rejected by the RPA. By setting the potential of the RPA to be just below the transport energy of the positrons, the beam can be filtered such that only unscattered positrons pass through the RPA. This can be seen in Figure 4 which demonstrates the path of both a scattered and unscattered particle through the apparatus. A positron that binds with an electron to form positronium is no longer confined by the magnetic field and carries on in a straight trajectory until it annihilates in flight or on contact with the wall. Thus, a positron that annihilates or binds with an electron to form positronium will not make it out of the scattering cell.

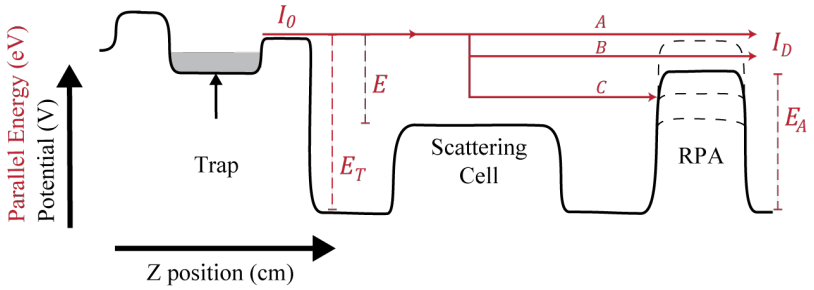

Figure 4: Plot of relative potentials in trap, scattering cell and RPA (not to scale). The initial beam intensity I_0, scattering energy E, detected intensity I_D and RPA threshold energy E_A are illustrated. Three example paths for a positron are shown for A: a positron that does not scatter, B: a positron that scatters but still has sufficient parallel energy to pass through the RPA and C: a positron that scatters such that it does not have sufficient parallel energy to pass the RPA.

Positrons that have sufficient energy ($> E_A$) to pass the RPA are then accelerated by an ~500 V potential into a multichannel plate detector. This amplifies the positron current which is measured and integrated to give the signal intensity. This integrated signal is proportional to the number of positrons in the post-RPA beam and is averaged over 100 positron pulses to improve statistical accuracy.

Assuming a projectile particle (in this case the positron) is removed from the beam upon interacting with a target particle (for example scattered away or annihilated), the grand total cross section σ_T is defined by the Beer-Lambert law,

$$\sigma_T = -\frac{1}{n_T l} \ln \frac{I_T}{I_0} \tag{7}$$

where l is the path length of the beam through the target particles, n_T is the numeric density of the target particles, I_T is the transmitted intensity and I_0 is the initial intensity of the beam.

The numeric density n_T of the target particles in equation (7) can be calculated using the ideal gas law

$$n_T = \frac{N}{V} = \frac{P}{kT} \tag{8}$$

where P is the pressure, k is Boltzmann's constant and T is the temperature of the target gas. For this experiment, the target gas is assumed to be at room temperature ($T = 300K$). To reduce the effect of multiple scattering, the pressure of the ethane gas in the scattering cell was adjusted so that ~10% of the positron beam is scattered by the gas. This makes the probability of double scattering just 0.5% so the effect of multiple scattering is ignored in this study.

To measure the initial intensity of the positron beam (I_{0R}), the RPA potential is set to 0 V so that no positrons are repelled. The potential of the scattering cell is set such that the positron energy E is just below the positronium formation energy of 4.7 eV. The transmitted intensity for each energy $I_m(E)$ can then be measured by setting the RPA voltage just below the transport energy such that only the unscattered positrons pass. Using the Beer-Lambert law from equation (7), the grand total cross section is

$$\sigma_T(E) = -\frac{1}{n_T l}\ln\frac{I_m(E)}{I_{0R}} \tag{9}$$

To separate the grand total cross section into positronium formation and difference components, the positrons taken from the beam through positronium formation must be distinguished from those that are scattered elastically or inelastically. As the apparatus is contained in a magnetic field, the scattered positrons remain in the beam with reduced parallel energy whilst those that annihilate or form positronium are removed from the beam entirely. Thus, an additional intensity measurement $I_0(E)$ is made for each energy with the RPA voltage again set to 0 which will count all positrons that do not form positronium in the scattering cell (any positrons that are scattered backwards are simply reflected off the trap potential and are still counted in the beam). A summary of all measurements required along with an example energy distribution of the positrons is shown in Figure 5.

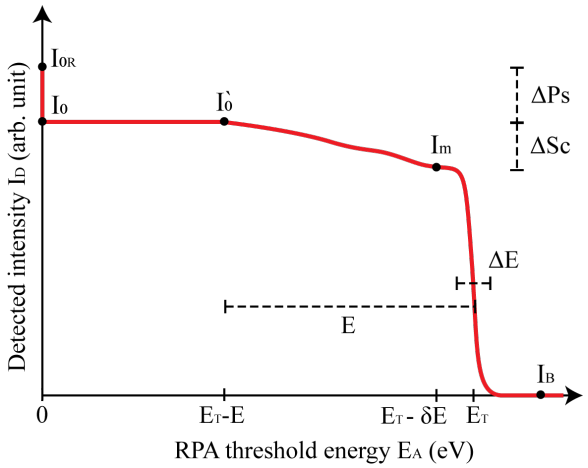

Figure 5: Diagram of intensity measurements required to calculate grand total, positronium and scattering cross sections. I_0, I_0' and I_m are measured for every scattering energy, whilst I_{0R} and I_B are measured once per scan.

The proportion of the grand total cross section due to positronium formation σ_{Ps} can then be approximated

$$\sigma_{Ps} = \frac{\Delta Ps}{\Delta Ps + \Delta Sc}\sigma_T = \frac{I_{0R} - I_0}{I_{0R} - I_m}\sigma_T \tag{10}$$

And likewise, the difference component σ_Δ

$$\sigma_\Delta = \frac{\Delta Sc}{\Delta Ps + \Delta Sc}\sigma_T = \frac{I_0 - I_m}{I_{0R} - I_m}\sigma_T \tag{11}$$

An additional systematic check is made by setting the voltage of the RPA to be the same as that of the scattering cell and recording the intensity I_0'. Ideally, $I_0 = I_0'$ as there should be no positrons with energy less than that required to enter the scattering cell reaching the RPA. However, it was found there is a small discrepancy between these values at low scattering energies where a large RPA potential is used. It is hypothesized that this is caused by a slight beam misalignment leading to a small number of positrons missing the detector. This misalignment would also affect the unscattered intensity measurement I_m which is at similar high RPA thresholds. A small correction (equal to the average $I_0 - I_0'$ difference at the minimum scattering energy of 1 eV) was added to

each I_m values to account for these lost positrons. This correction is similar in magnitude to the reported statistical uncertainties.

An additional baseline zero measurement I_B is taken for the intensity by setting the RPA slightly higher than the transport energy E_T such that all positrons are repelled. This is averaged across all scans and subtracted from each of the measurements to provide a consistent zero point.

The predominant source of uncertainty is the statistical fluctuations in the number of positrons per pulse. Thus, the scans described above were repeated at least 1000 times. There are two methods to then combine the results from each scan; Either calculate an individual cross section for each scan and then average them or average the intensity measurements across scans and calculate a cross section from the average. The results from the two methods differed significantly (varying by double the reported uncertainty) as the logarithm in equation (9) significantly skews the distribution. This effect is visualized in Figure 6 where it is evident that lower values of x in the distribution affect the mean disproportionately relative to higher values. Since the inherent statistical uncertainty is in the measured beam intensity, it was decided that averaging the intensity values prior to calculating the cross section is preferable to avoid skewing the distribution. This requires first normalizing the magnitude of each measurement such that $I_{0R} = 1$ for all scans to account for varying pressure and moderator efficiency over the duration of the experiment. The pressure was also averaged across all scans prior to calculating the numeric density of the gas. The uncertainty in the intensity measurements is calculated using the statistical uncertainty in the mean which is then propagated through the cross section calculation. The uncertainty in pressure and scattering cell length were also considered, however the statistical uncertainty was dominant in the results.

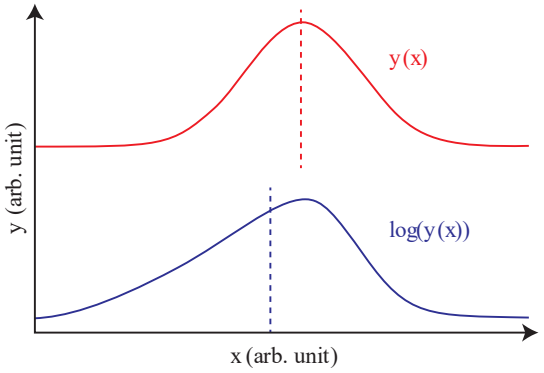

Figure 6: Normal and log-normal distributions. The mean of each distribution is marked with a dashed line.

Results

The measured grand total cross section along with the positronium formation and difference cross calculated using the techniques described above are depicted in Figure 7 with comparison to the previous results of Chiari and Floeder. The code used to calculate and plot the cross sections is available in a publicly accessible git repository (https://github.com/ryanstocks00/positron-cross-section).

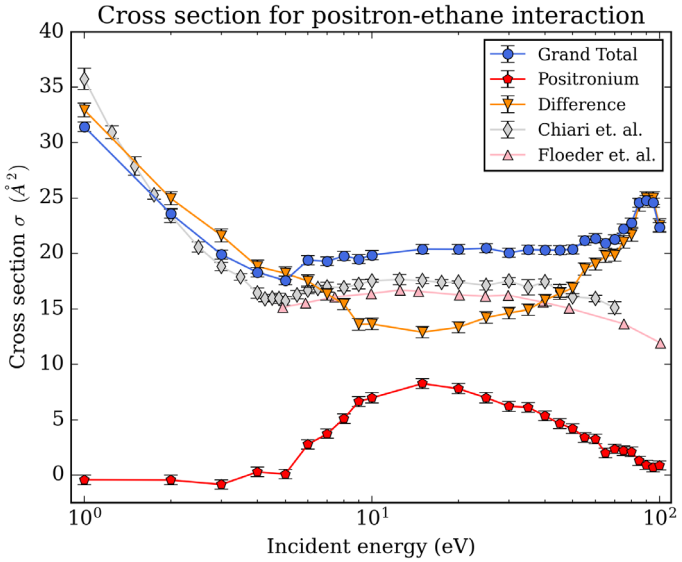

Figure 7: Measured grand total, positronium formation and difference cross sections of the positron-ethane interaction with comparison to previous grand total cross section measurements by Chiari et. al. [6] and Floeder et. al. [7]. Each datapoint has been averaged over ~1500 scans with error bars representing the statistical uncertainty in the mean.The lines connecting adjacent datapoints are purely a visual aid for the reader.

It is evident in Figure 7 that there is a substantial difference between the measured grand total cross section and the measurements of both previous studies. Upon further investigation, it was found that the measured cross sections were shifting over the duration of the experiment. This effect was most apparent at 90 eV, with the grand total cross section increasing by almost 10 $Å^2$ after 23 hours. This coincides with the unexpected peak in the cross section, indicating a significant systematic error. The effect was consistent across multiple experiments and appeared to be reset by flushing the ethane from the scattering cell. Numerous potential causes were assessed and eventually the cause was determined to be an ionizing pressure gauge between the scattering cell and the RPA. It is hypothesized that the pressure gauge was ionizing residual particles over time which were then charging different sections of the apparatus. This then interfered with the particle transport getting worse the longer the experiment ran. When the gas is removed, the ion flux is reduced so any charged areas would discharge, resetting the effect. Disabling the pressure gauge reduced the effect significantly and removed the unexpected bump. The experiment was repeated with the pressure gauge disabled and the new results are displayed in Figure 8.

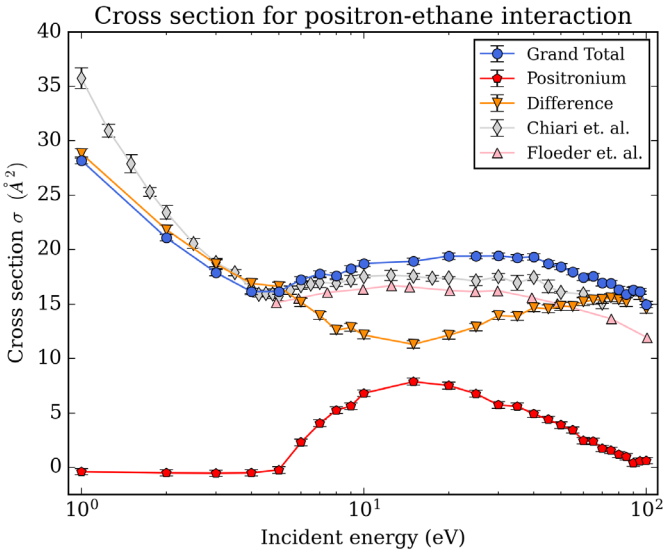

Figure 8: Same as Figure 7 but with ionizing pressure gauge disabled.

The measured grand total cross sections are consistently below those of Chiari et. al. in the 1 to 4 eV range, whilst they are consistently 1 to 3 $Å^2$ higher in the 6 to 100 eV range. The positronium formation cross section is zero until ~5 eV where it climbs rapidly to a cross section of 7.9 ± 0.3 $Å^2$ at 15 eV just above the ionisation energy before decreasing back to just 0.6 ± 0.3 $Å^2$ at 90 to 100 eV.

Unfortunately, an additional systematic error was present with the measured grand total cross section now decreasing over time. This was most evident at low energies, with the cross section dropping by 7 $Å^2$ over the 19 $hour$ experiment. The effect was much less significant at higher energies, dropping at most 3 $Å^2$ in the range from 15 eV to 100 eV indicating an absolute error around ± 1.5 $Å^2$ from the mean in this region. The statistical uncertainty in each measurement is ~0.3 $Å^2$ so the systematic error is significant (approximately five times the statistical uncertainty). This means that further work will be required to eliminate systematic errors before publishable results are obtained, however analysis of these results can still provide insight.

Discussion

A significant challenge for positron scattering experiments is distinguishing forward scattered positrons that are elastically scattered at a small angle from the rest of the beam. All experiments are limited to some angular acceptance and any positrons scattered within that angle can't be distinguished from the incident beam. As such the measured elastic scattering cross section is always a lower limit of the actual elastic scattering cross section. In this experiment, the parallel energy acceptance remains constant ($\delta E = 80$ meV). The angular acceptance thus ranges from 1.8° at 100 eV to 16° at 1 eV as calculated using equation (5). In contrast, the experiments of Floeder et. al and Chiari et. al. rely on a geometric angular discrimination that is consistent throughout the energy range.

The reported angular acceptances are $\delta\theta \sim 5.7°$ [7] and $\delta\theta \sim 4°$ [6] respectively. The cross over from below the previous experimental measurements to above is thus expected due to the inferior angular acceptance at low energies and superior angular acceptance at high energies. It has been shown previously that elastic scattering cross sections are often forward peaked, particularly at high energies so the small difference in angular discrimination can be quite significant [18].

The improved energy resolution may also contribute to the reduced cross section at low energies. Chiari et. al. reports an energy width of ~0.25 eV (FWHM) compared to just 0.05 eV in this study. A wider energy distribution may result in measuring higher cross sections at low energies as positrons at the bottom end of the band will contribute more than those at the top end of the band since the cross section rises towards zero energy. This is unlikely to be as significant as the difference in angular acceptance but likely exacerbates the effect.

The positronium formation cross section is as expected, with no positronium formation below the estimated 4.7 eV threshold. The shape is consistent with the positronium formation cross sections measured for other molecules such as H_2O [19] rising rapidly to a peak and then decreasing again at higher energies. Interestingly, the difference cross section increases again whilst the positronium formation cross section declines. This is likely due to the positron having sufficient energy to ionize or excite higher energy states of the ethane molecule when scattering inelastically which would increase the inelastic cross section. The introduction of ionization at $11.5\ eV$ is likely a significant component of this effect.

As described above, there are unfortunately still systematic errors in the final results. Resolving these errors was beyond the time scope of this project, however subsequent work has been conducted by the group to attempt to rectify them. This included baking the apparatus to remove contamination and reducing the gain of the detector to avoid saturation. Preliminary tests are promising, however additional experimentation has not yet been possible.

Once the systematic errors have been resolved and publishable grand total cross section results have been achieved, there is significant room for further work expanding the set of experimental data using the current apparatus. The total cross section does not provide a complete picture of the scattering process, and past research has shown that there can be good agreement between experiment and theory for the total cross section with little alignment in the underlying differential cross section [20]. It is relatively simple to modify the current experimental setup to instead measure the elastic differential cross section by adding additional measurements within the scattered energy range (I_0' to I_m). This would correspond to different parallel energies after scattering which can then be converted to a scattered angle. Similar approaches have been developed to measure total inelastic cross sections using the same apparatus by varying the strength of the magnetic field [21]. A long-term goal of the project is to probe the inelastic cross sections around the vibrational modes associated with the positron-ethane bound states which may provide greater insight into the underlying processes.

Conclusion

Measurements of the grand total, positronium formation, and difference cross sections for a positron-ethane interaction in the energy range 1 to 100 eV were reported. The new grand total cross section results are consistent with those of Chiari et. al. [6] and Floeder et. al. [7]. The positronium/annihilation cross section is zero below the calculated positronium formation threshold of 4.7 eV and peaks at 15 eV reaching 7.9 ± 0.3 Å^2 before declining at higher energies. The difference cross section is maximal at low energies, decreasing until the peak of the positronium formation cross section and then increasing again at higher energies. This increase is likely due to having sufficient energy to inelastically excite higher energy states (e.g., electronic excited states) or ionize the ethane molecule. Unfortunately, systematic errors are present in the reported measurements as the grand total cross section was observed to shift over the duration of the experiment. Further work is required to reduce these systematic errors and obtain publishable results; however, this was beyond the time scope of this project. Once these errors have been resolved, there will be improved confidence in the operation of the apparatus and higher precision measurements of the inelastic scattering around the vibrational modes can be conducted to probe the bound states and resonances discussed in the introduction.

References

[1] M. Aguilar et. al., "Towards Understanding the Origin of Cosmic-Ray Positrons," *Phys. Rev. Lett.,* vol. 122, no. 4, p. 9, 2019.

[2] R. W. Siegel, "Positron Annihilation Spectroscopy," *Annual Review of Materials Science,* vol. 10, no. 1, pp. 393-425, 1980.

[3] M. M. Ter-Pogossian, M. E. Phelps, E. J. Hoffman and N. A. Mullani, "A Positron-Emission Transaxial Tomograph for Nuclear Imaging (PETT)," *Radiology,* vol. 114, no. 1, pp. 89-98, 1975.

[4] S. J. Gilbert, L. D. Barnes, J. P. Sullivan and C. M. Surko, "Vibrational-Resonance Enhancement of Positron Annihilation in Molecules," *Phys. Rev. Lett.,* vol. 88, no. 4, p. 4, 2002.

[5] A. R. Swann and G. F. Gribakin, "Positron Binding and Annihilation in Alkane Molecules," *Phys. Rev. Lett.,* vol. 123, no. 11, 2019.

[6] L. Chiari et. al., "Cross sections for positron scattering from ethane," *Physical Review A,* vol. 87, 2013.

[7] K. Floeder, D. Fromme, W. Raith, A. Schwab and G. Sinapius, "Total cross section measurements for positron and electron scattering on hydrocarbons between 5 and 400 {eV}," *Journal of Physics B: Atomic and Molecular Physics,* vol. 18, no. 16, pp. 3347-3359, 1985.

[8] P. A. M. Dirac, "The quantum theory of the electron," *Royal Society,* vol. 117, no. 778, pp. 610-624, 1928.

[9] C. D. Anderson, "The Positive Electron," *Phys. Rev.,* vol. 43, no. 6, pp. 491-494, Mar 1933.

[10] G. B. Andresen et. al., "Trapped antihydrogen," *Nature,* vol. 468, no. 7324, pp. 673-676, 2010.

[11] M. Ahmadi et. al., "Observation of the 1S–2S transition in trapped antihydrogen," *Nature,* vol. 541, no. 7638, pp. 506-510, 2017.

[12] T. Shimanouchi, "Tables of Molecular Vibrational Frequencies Consolidated Volume I," *National Bureau of Standards,* pp. 1-160, 1972.

[13] S. G. Karshenboim, "PRECISION STUDY OF POSITRONIUM: TESTING BOUND STATE QED THEORY," *International Journal of Modern Physics A,* vol. 19, no. 23, pp. 3879-3896, 2004.

[14] M. J. S. Dewar and S. D. Worley, "Photoelectron Spectra of Molecules. I. Ionization Potentials of Some Organic Molecules and Their Interpretation," *The Journal of Chemical Physics,* vol. 50, no. 2, pp. 654-667, 1969.

[15] S. Berko and H. N. Pendleton, "Positronium," *Annual Review of Nuclear and Particle Science,* vol. 30, no. 1, pp. 543-581, 1980.

[16] J. P. Sullivan, A. Jones, P. Caradonna, C. Makochekanwa and S. J. Buckman, "A positron trap and beam apparatus for atomic and molecular scattering experiments," *Review of Scientific Instruments,* vol. 79, no. 11, 2008.

[17] R. Greaves and C. Surko, "Solid neon moderator for positron-trapping experiments," *Canadian Journal of Physics,* vol. 74, pp. 445-448, 2011.

[18] J. P. Sullivan, C Makochekanwa, A. Jones et. al., "Forward angle scattering effects in the measurement of total cross sections for positron scattering," *Journal of Physics B: Atomic, Molecular and Optical Physics,* vol. 44, no. 3, 2011.

[19] C. Makochekanwa, A. Bankovic, W. Tattersall, A. Jones, P. Caradonna, D. S. Slaughter, K. Nixon, M. J. Brunger, Z. Petrovic, J. P. Sullivan and S. J. Buckman, "Total and positronium formation cross sections for positron scattering from H2O and HCOOH," *New Journal of Physics,* vol. 11, no. 10, 2009.

[20] D. Edwards, D. Stevens, Z. Cheong et. al., "Positron scattering from pyrazine," *Phys. Rev. A,* vol. 104, no. 4, 2021.

[21] J. P. Sullivan, S. J. Gilbert, J. P. Marler, R. G. Greaves, S. J. Buckman and C. M. Surko, "Positron scattering from atoms and molecules using a magnetized beam," *Phys. Rev. A,* vol. 66, no. 4, 2002.